

# Robust Coordinated Control for a Type of Hypersonic Aircraft

Mu Jinzhen<sup>1,2</sup>, Wang Yuhui<sup>1\*</sup>, Wu Qingxian<sup>1</sup>, Ying Junyu<sup>1</sup>

1. College of Automation Engineering, Nanjing University of Aeronautics and Astronautics, Nanjing 211106, P. R. China;

2. Shanghai Aerospace Control Technology Institute, Shanghai 201109, P. R. China

(Received 23 June 2017; revised 2 December 2017; accepted 16 January 2018)

**Abstract:** We investigate couplings between variables of attitude dynamics for a hypersonic aircraft, and present a nonlinear robust coordinated control scheme for it. First, we design three kinds of coordinated factors to restrain the strong couplings. Then, we use projection mapping to estimate the uncertain nonlinear functions of the aircraft. Combining the coordinated factors and the designed control laws, we obtain a coordinated torque and assign it to the control deflection commands by using the allocation matrix. A stability analysis demonstrates that all the signals of the closed-loop system are uniformly and fully bounded. Finally, the robust coordinated performance of the designed scheme is verified through numerical simulations.

**Key words:** hypersonic flight vehicle; attitude control; coordinated control; robustness; adaptive control

**CLC number:** V448.2      **Document code:** A      **Article ID:** 1005-1120(2018)06-1000-10

## 0 Introduction

Attitude control is critical to stability and trajectory control for hypersonic aircraft<sup>[1-3]</sup>, but it is challenged by many factors, including strong couplings, complex nonlinearities, uncertainties, and limited control surface deflections and thrusts<sup>[4-8]</sup>.

Recent studies concentrate on three aspects. First, accurate control model caught researchers' attentions. Refs. [9-12] designed online neural network adaptive control laws based on feedback linearization. Feedback linearization methods, however, heavily depend on model accuracy and can hardly guarantee good control performance with model uncertainties and external disturbances. Subsequently, linear robust methods were introduced. Ref. [13] proposed an intelligent controller based on the fuzzy dynamic characteristic modeling. Ref. [14] presented a robust control system featuring fixed feedback gains and applied multi-model eigen structure assignment with respect to the specific tasks of a hypersonic vehicle. Although these two methods could effectively

achieve robustness, their linearization steps may cause considerable modeling errors and uncertainties. Thus, nonlinear robust control methods emerged. Sliding mode control has good adaptability and high robustness for system disturbances and parameter perturbations, and has been successfully applied to industrial control<sup>[15-17]</sup>. Ref. [18] designed sliding mode controller to improve the robustness. Then, Ref. [19] presented a disturbance observer to estimate the unknown disturbance of a hypersonic vehicle.

Although coupling problems are frequently mentioned in the above studies, none of them has proposed theories to directly solve them. Strong couplings can cause complicated interactions between variables which consequently lead to more complex behaviors of aircraft with more variations and uncertainties. Some scholars have noticed this and started exploratory studies on coordinated controllers<sup>[20-24]</sup>. Ref. [20] presented a nonlinear longitudinal model for a hypersonic vehicle, which could describe the inertial coupling effects between the pitch dynamics. Ref. [21]

\*Corresponding author, E-mail address: wangyh@nuaa.edu.cn.

proposed an assessment of the interactions among the airframe, engine, and structural dynamics and designed a highly integrated airframe engine control system to deal with the strong couplings. These studies, however, focused on analysis of strong couplings without any expressions. Therefore, inspired by previous studies, we present a nonlinear robust coordinated control scheme for hypersonic aircraft, which highlights certain privileges as follows.

(1) Inspired by the ideas in Refs. [25-26], we categorize the coupling relationships of the variables in three types: Attitude coupling, inertia coupling and aerodynamic coupling.

(2) Based on the three coupling types, a series of novel coordinated factors are obtained.

(3) Uncertain parameters are integrated into a vector for the convenience of online estimation, so that we can construct an adaptive estimator and enhance the robustness of the controller. We also introduce a nonlinear observer to estimate the disturbance in the control-coefficient matrix.

(4) We introduce designed coordinated factors to deduce the coordinated moment of force.

## 1 Hypersonic Aircraft Model

Ignoring the flexibility effects of the structure, the wind, the earth rotation, and the earth curvature, the attitude dynamic model of a hypersonic aircraft<sup>[3]</sup> containing aerodynamic parameters' CFD (computational fluid dynamics) data can be described by the following nonlinear equations<sup>[3, 27-28]</sup>

$$\begin{cases} \dot{\boldsymbol{\Omega}} = \mathbf{f}_s + \mathbf{g}_s \boldsymbol{\omega} \\ \dot{\boldsymbol{\omega}} = \mathbf{f}_f + \mathbf{g}_f \mathbf{M}_c \end{cases} \quad (1)$$

where  $\boldsymbol{\Omega} = [\alpha, \beta, \mu]^\top$ ,  $\mathbf{f}_s = [f_a, f_\beta, f_\mu]^\top$ ,  $\boldsymbol{\omega} = [p, q, r]^\top$ ,  $\mathbf{f}_f = [f_p, f_q, f_r]^\top$ , and

$$\begin{aligned} f_a &= \frac{1}{MV \cos \beta} (-\bar{q} SC_{L,a} + Mg \cos \gamma \cos \mu) \\ f_\beta &= \frac{1}{MV} (\bar{q} SC_{Y,\beta} + Mg \cos \gamma \sin \mu) \\ f_\mu &= \frac{1}{MV} \bar{q} SC_{Y,\beta} \tan \gamma \cos \mu + \frac{1}{MV} \bar{q} SC_{L,a} \cdot \\ & (\tan \gamma \sin \mu + \tan \beta) - \frac{g}{V} \cos \gamma \cos \mu \tan \beta \end{aligned} \quad (2)$$

$$\mathbf{g}_s = \begin{bmatrix} -\cos \alpha \tan \beta & 1 & -\sin \alpha \tan \beta \\ \sin \alpha & 0 & -\cos \alpha \\ \cos \alpha \sec \beta & 0 & \sin \alpha \sec \beta \end{bmatrix} \quad (3)$$

$$f_p = \frac{1}{I_{xx}} (l_{\text{aero}} + (I_{yy} - I_{zz})qr - \dot{I}_{xx}p)$$

$$f_q = \frac{1}{I_{yy}} (m_{\text{aero}} + (I_{zz} - I_{xx})pr - \dot{I}_{yy}q) \quad (4)$$

$$f_r = \frac{1}{I_{zz}} (n_{\text{aero}} + (I_{xx} - I_{yy})pq - \dot{I}_{zz}r)$$

$$\mathbf{g}_f = \begin{bmatrix} g_l^p & 0 & 0 \\ 0 & g_m^q & 0 \\ 0 & 0 & g_n^r \end{bmatrix} \quad (5)$$

$$\begin{aligned} l_{\text{aero}} &= \bar{q} Sb [C_{l,\beta} \beta + C_{l,p} pb / (2V) + C_{l,r} rb / (2V)] \\ m_{\text{aero}} &= \bar{q} Sc [C_{m,\alpha} + C_{m,q} qc / (2V)] + \\ & X_{cg} \bar{q} S (C_{D,\alpha} \sin \alpha + C_{L,\alpha} \cos \alpha) \\ n_{\text{aero}} &= \bar{q} Sb [C_{n,\beta} \beta + C_{n,p} pb / (2V) + C_{n,r} rb / (2V)] + \\ & X_{cg} \bar{q} SC_{Y,\beta} \beta \end{aligned} \quad (6)$$

where  $\alpha$ ,  $\beta$ ,  $\mu$  are the angle of attack, the sideslip angle, and the bank angle, respectively;  $p$ ,  $q$ ,  $r$  the roll rate, the pitch rate, and the yaw rate, respectively;  $\mathbf{M}_c = \mathbf{g}_{f\delta} \mathbf{u}$ , where  $\mathbf{g}_{f\delta} \in \mathbf{R}^{3 \times 3}$  is the fast loop allocation matrix,  $\mathbf{u} = [\delta_e, \delta_a, \delta_r]^\top$ , where  $\delta_e, \delta_a, \delta_r$  are the deflection angles of elevator, aileron, and rudder, respectively;  $M$  is the vehicle mass;  $V$  the velocity;  $\bar{q}$  the dynamic pressure;  $S$ ,  $c$ ,  $b$  are the reference area, the reference length, and reference width, respectively;  $I_{xx}$ ,  $I_{yy}$ ,  $I_{zz}$  the roll, the yaw, and pitch moments of inertia, respectively; and  $X_{cg}$  is the longitudinal distance from the momentum reference to the vehicle. The basic parameters and aerodynamic coefficients of the vehicle can be obtained in Refs. [3, 27-28].

**Remark 1** Due to the complicated nonlinear dynamics of hypersonic aircraft, it is difficult to study directly the rigid-flexible coupling problem without the knowledge of the rigid couplings. Ref. [29] investigated a double-loop coordinated decoupling control to deal with the couplings, but it lacks explicit investigation on the effect of the flexible dynamics on the attitude system. By using statistical sampling method, a series of coupling degrees were provided based on rigid-body

dynamics<sup>[30-31]</sup>. If considering the flexible coupling dynamics, the flexibility variables should be involved in the method<sup>[30-31]</sup>, and the coupling degrees must be calculated online. But the statistical sampling method<sup>[30-31]</sup> does not support online computing. In Refs. [32-34], the flexible coupling effects were modeled as a kind of unknown disturbance, then a coupling-observer-based compensator was proposed to restrict the flexible effects on pitch rate. If considering all flexible dynamics, the control method may cause high-frequency oscillations. Based on a rigid-body dynamic model, Refs. [35-36] introduced a novel coupling analysis index to describe the coupling relationships among the variables. But if the flexible coupling dynamics was considered, the method<sup>[35-36]</sup> would not be directly applied to design the controller, because the couplings of the attitude channels have positive and negative polarities. To analyze the strong coupling characteristics of a hypersonic aircrafts Ref. [25] defined the nonlinear degree based on rigid-body dynamics, and then introduced it to characterize the rigid-flexible couplings. Ref. [25] provides a new direction for further study. Therefore, dealing with the couplings of the flight state variables based on the rigid-body dynamics is the first step of our research.

## 2 Coupling Analysis

Obviously, strong nonlinear couplings exist in the above mentioned attitude systems (1)–(6), and they can be described as the following coupling types.

### (1) Attitude coupling

To consider the effects of the angular rates on the attitude angles while neglecting  $f_s$  in the first sub-equation of Eq. (1), we describe the attitude coupling as

$$\begin{aligned}\dot{\alpha} &= -\tan\beta(p\cos\alpha + r\sin\alpha) \\ \dot{\beta} &= p\sin\alpha - r\cos\alpha \\ \dot{\mu} &= \sec\beta(p\cos\alpha + r\sin\alpha)\end{aligned}\quad (7)$$

### (2) Inertia coupling

If the effects of  $l_{\text{aero}}, m_{\text{aero}}, n_{\text{aero}}$  on the angular

rates are ignored, the inertia coupling which among the channels of the roll, the pitch, and the yaw in Eq. (4) can be described as

$$\begin{aligned}f_p &= (I_{yy} - I_{zz})qr - \dot{I}_{xx}p \\ f_q &= (I_{zz} - I_{xx})pr - \dot{I}_{yy}q \\ f_r &= (I_{xx} - I_{yy})pq - \dot{I}_{zz}p\end{aligned}\quad (8)$$

### (3) Surface deflection coupling

According to Refs. [27-28], it can be known that there always exists surface deflection coupling due to the complicated aerodynamics of hypersonic aircraft, then combing the expression of  $g_{f\delta}$  in Refs. [23, 28], the surface deflection coupling can be described as

$$\begin{aligned}g_l &= \bar{q}Sb(C_{l,\delta_a} + C_{l,\delta_r}) \\ g_m &= \bar{q}Sc(C_{m,\delta_a} + C_{m,\delta_r}) \\ g_n &= \bar{q}Sb(C_{n,\delta_a} + C_{n,\delta_r})\end{aligned}\quad (9)$$

Obviously, the above equations show that there exist complex coupling relationships within hypersonic aircraft. In hypersonic speed, the above couplings are more complex, resulting in aileron reversal operation phenomenon and system uncertainties, or even the system instability. Some scholars have put forward decoupling methods<sup>[29]</sup>. But they are not an effective way for hypersonic aircraft, because the decoupling methods may change the intrinsic nonlinear characteristics of the vehicles. Therefore, Ref. [30] presented a new scheme to describe the coupling relationships in mathematics, and the linear coupling degree could be obtained by using statistical sampling method. However, the coupling matrices provided in Ref. [30] are linear, which is not accurate enough to describe the complex couplings of the hypersonic flight vehicles. Therefore, we propose a novel method to describe the nonlinear couplings of the aircraft and design a coordinated attitude controller to coordinate the attitude dynamics.

## 3 Design of Coordinated Factors

### 3.1 Coordinated factors for attitude coupling

For flight dynamics, the sideslip angle may

cause unstable flight. Therefore,  $\dot{\beta}$  is set as zero (Eq. (7)), that is,  $p \sin \alpha - r \cos \alpha = 0$ . Then  $r = p \tan \alpha$  can be obtained. Thus, the coordinated factor can be designed as

$$\lambda_{r_1} = k_1 p \tan \alpha \quad (10)$$

where  $k_1 > 0$  is a designed parameter.

In contrast to the unavailable coupling between  $\alpha$  and  $\beta$ , the coupling between  $\alpha$  and  $\mu$  can be regarded as an available coupling when the aircraft is flying at a very small angle of attack. Then we have

$$\begin{cases} p \cos \alpha + r \sin \alpha = p & \alpha = 0 \\ p \cos \alpha + r \sin \alpha \leq p + \rho r & \alpha > 0 \\ p - \sigma < p \cos \alpha + r \sin \alpha & \alpha < 0 \end{cases} \quad (11)$$

where  $\rho$  is a positive constant and  $\sin \alpha < \rho$ , and  $\sigma$  a positive constant,  $\sigma > |\sin \alpha|$ . Then the strong attitude coupling relationships in Eq. (7) can be described as  $p - \sigma r < p \leq p \cos \alpha + r \sin \alpha \leq p + \rho r$ . In order to increase the damping torque,  $\beta$  is introduced as feedback to the rudder channel. Thus, the coordinated factor is selected as

$$\lambda_{r_2} = k_2 \beta + k_3 \frac{p(1 - \cos \alpha)}{\sin \alpha + \Delta_a} \quad (12)$$

where  $\Delta_a$  is a designed parameter to avoid the singularity of Eq. (12),  $|\sin \alpha| \neq \Delta_a$ , and  $k_2, k_3 > 0$  are designed parameters.

Combining Eq. (10) and Eq. (12), the attitude coupling coordinated factor can be described as

$$\lambda_r = \lambda_{r_1} + \lambda_{r_2} = k_1 p \tan \alpha + k_2 \beta + k_3 \frac{p(1 - \cos \alpha)}{\sin \alpha + \Delta_a} \quad (13)$$

### 3.2 Coordinated factors for inertia coupling

The sideslip angle tends to diverge because of the inertial coupling torques, so the terms  $(I_{yy} - I_{zz})qr$ ,  $(I_{zz} - I_{xx})pr$ , and  $(I_{xx} - I_{yy})pq$  in Eq. (8) cannot be ignored. Taking the yaw inertia as an example, when the inertia is in critical state,  $f_r + f'_r + f'_\beta = 0$ , where  $f_r$  is the yaw inertia coupling torque;  $f'_r$  the yaw damping torque, and  $f'_\beta$  the yaw steady torque. With the accumulation of inertia coupling, the inertia coupling torque will be greater than the damping torque and the steady torque, which will lead to the sideslip angle unstable. To reduce the negative impacts of the in-

ertia coupling, the damping torque and steady torque should be increased to restrain the trend. The basic idea of the coordinated control is to introduce  $\beta$  and  $r$  into the aileron loop to increase the damping torque,  $\beta$  and  $q$  into the rudder loop to increase the steady torque, and  $\alpha$  and  $p$  into the elevator loop to increase the damping torque. Thus, the inertia coupling coordinated factors are designed as

$$\begin{cases} \lambda_e = k_4 \alpha + k_5 p \\ \lambda_a = k_6 \beta + k_7 r \\ \lambda_{r_3} = k_8 \beta + k_9 q \end{cases} \quad (14)$$

where  $k_4, k_5, k_6, k_7, k_8 > 0$  are designed parameters.

### 3.3 Coordinated factors for surface deflection

With consideration of the flight dynamics of hypersonic aircraft, Ref. [30] provided a method to describe the coupling degree in mathematics. But by analysis, the coupling degree should reasonably describe the couplings between the rudder deflection and aileron deflection<sup>[31]</sup>.

Thus, the surface deflection coupling degree is chosen as<sup>[31]</sup>

$$E = \frac{C_{x'}^{\delta_r}}{C_{x'}^{\delta_a}} \times 100\% \quad (15)$$

where  $E$  represents the surface deflection degree between the aileron deflection and rudder deflection. It indicates that the surface deflection degree is determined by the aerodynamic shape and flight state. And

$$C_{x'}^{\delta_r} = \frac{S_{cwr} S_{cw}}{S^2} \frac{y_{cwr}}{L} \xi \cos \chi \quad (16)$$

$$C_{x'}^{\delta_a} = \frac{1}{2} \left\{ n \frac{(\eta_k + 1)(1 - \bar{D})^2}{\eta_k + 1 - 2\bar{D}} [\bar{D} + (1 - \bar{D})f] \right\} \quad (17)$$

where  $S_{cwr}$ ,  $S_{cw}$  are the rudder area and the vertical area, respectively;  $S$ ,  $L$  are the reference area and reference length;  $y_{cwr}$  is the distance from the rudder surface center to the vertical axis;  $\chi$  the sweep back angle;  $\xi$  the correction factor;  $n$  the relative efficiency of the aileron;  $\eta_k$ ,  $\bar{D}$  are the exposed wing ratio and diameter ratio, respectively; and  $f$  is the ratio between the distance from exposed wing root profile to center pressure and

wing length. In Eq. (17),  $S_{cwr} \leq S$ ,  $S_{cw} \leq S$ ,  $y_{cwr} \leq L$ ,  $0 < \xi \leq 1$ ,  $0 < \cos \chi \leq 1$ , and  $C_{x^{\delta}} \geq 1$ . Thus, the surface coordinated deflection strategy is chosen as

$$\delta_a = E\delta_r \quad 0 < E \leq 1 \quad (18)$$

Based on Eqs. (13), (14), the hypersonic vehicle attitude coordinated factors are given as

$$\begin{cases} \lambda_e = k_4 \alpha + k_5 q \\ \lambda_r = \lambda_{r1} + \lambda_{r2} + \lambda_{r3} \\ \lambda_a = k_6 \beta + k_7 p \end{cases} \quad (19)$$

where  $k_i > 0, i = 1, \dots, 7$  is designed parameter.

## 4 Coordinated Attitude Controller Design

By introducing the uncertain parameters, a hypersonic aircraft attitude dynamics can be re-written as

$$\dot{\boldsymbol{\Omega}} = \mathbf{f}_1 + \boldsymbol{\Psi}^T \boldsymbol{\theta}_\Omega + \mathbf{g}_\omega \boldsymbol{\omega} \quad (20)$$

$$\dot{\boldsymbol{\omega}} = \boldsymbol{\Xi}^T \boldsymbol{\theta}_\omega + \mathbf{g}_f \mathbf{M}_c + \mathbf{d}$$

where  $\mathbf{d}$  is the external perturbation, and

$$\boldsymbol{\theta}_\Omega = [\boldsymbol{\theta}_1^T \quad \boldsymbol{\theta}_2^T \quad \boldsymbol{\theta}_3^T]_{4 \times 1}^T, \boldsymbol{\theta}_\omega = [\boldsymbol{\theta}_4^T \quad \boldsymbol{\theta}_5^T \quad \boldsymbol{\theta}_6^T]_{17 \times 1}^T \quad (21)$$

$$\boldsymbol{\theta}_1 = C_{L,a}, \boldsymbol{\theta}_2 = C_{Y,\beta}, \boldsymbol{\theta}_3 = [C_{Y,\beta}, C_{L,a}]^T$$

$$\boldsymbol{\theta}_4 = \begin{bmatrix} \frac{I_{xx} - I_{yy}}{I_{zz}} & \frac{\dot{I}_{zz}}{I_{zz}} & \frac{C_{n,\beta}}{I_{zz}} & \frac{C_{n,p}}{I_{zz}} & \frac{C_{n,r}}{I_{zz}} & \frac{C_{\gamma,\beta}}{I_{zz}} \end{bmatrix}^T$$

$$\boldsymbol{\theta}_5 = \begin{bmatrix} \frac{I_{zz} - I_{xx}}{I_{yy}} & \frac{\dot{I}_{yy}}{I_{yy}} & \frac{C_{m,a}}{I_{yy}} & \frac{C_{m,q}}{I_{yy}} & \frac{C_{D,a}}{I_{yy}} & \frac{C_{L,a}}{I_{yy}} \end{bmatrix}^T$$

$$\boldsymbol{\theta}_6 = \begin{bmatrix} \frac{I_{yy} - I_{zz}}{I_{xx}} & \frac{\dot{I}_{xx}}{I_{xx}} & \frac{C_{l,\beta}}{I_{xx}} & \frac{C_{l,p}}{I_{xx}} & \frac{C_{l,r}}{I_{xx}} \end{bmatrix}^T \quad (22)$$

$$\boldsymbol{\Psi}_1(x) = -\frac{\bar{q}S}{MV \cos \beta}, \boldsymbol{\Psi}_2 = -\frac{\bar{q}S \beta \cos \beta}{MV}$$

$$\boldsymbol{\Psi}_3 = \begin{bmatrix} \frac{\bar{q}S \beta \tan \gamma \cos \mu \cos \beta}{MV} & \frac{\bar{q}S (\tan \gamma \sin \mu + \tan \beta)}{MV} \end{bmatrix}^T \quad (23)$$

$$\boldsymbol{\Xi}_1(x) = \begin{bmatrix} qr & -p & \bar{q}Sb\beta & \frac{\bar{q}Sb^2 p}{2V} & \frac{\bar{q}Sb^2 r}{2V} \end{bmatrix}^T$$

$$\boldsymbol{\Xi}_2(x) = \begin{bmatrix} pr & -q & \bar{q}Sc & \frac{\bar{q}Sc^2 q}{2V} \\ X_{cg} \bar{q}S \sin \alpha & X_{cg} \bar{q}S \cos \alpha \end{bmatrix}^T \quad (24)$$

$$\boldsymbol{\Xi}_3(x) = \begin{bmatrix} pq & -r & \bar{q}Sb\beta & \frac{\bar{q}Sb^2 p}{2V} & \frac{\bar{q}Sb^2 r}{2V} & X_{cg} \bar{q}S \beta \end{bmatrix}^T$$

$$\boldsymbol{\Psi} = \begin{bmatrix} \boldsymbol{\Psi}_1 & 0 & 0 \\ 0 & \boldsymbol{\Psi}_2 & 0 \\ \mathbf{0}_{2 \times 1} & \mathbf{0}_{2 \times 1} & \boldsymbol{\Psi}_3 \end{bmatrix}_{4 \times 3}$$

$$\boldsymbol{\Xi} = \begin{bmatrix} \boldsymbol{\Xi}_1 & \mathbf{0}_{5 \times 1} & \mathbf{0}_{5 \times 1} \\ \mathbf{0}_{6 \times 1} & \boldsymbol{\Xi}_2 & \mathbf{0}_{6 \times 1} \\ \mathbf{0}_{6 \times 1} & \mathbf{0}_{6 \times 1} & \boldsymbol{\Xi}_3 \end{bmatrix}_{17 \times 3} \quad (25)$$

$$\mathbf{f}_1 = \begin{bmatrix} \frac{g \cos \gamma \cos \mu}{V \cos \beta} \\ \frac{g \cos \gamma \sin \mu}{V} \\ -\frac{g \cos \gamma \cos \mu \tan \beta}{V} \end{bmatrix} \quad (26)$$

Then, the control objective is that the attitude angle  $\boldsymbol{\Omega}$  can track the desired signal  $\boldsymbol{\Omega}_c$ , then the tracking error vector can be defined as  $\mathbf{e}_1 = \boldsymbol{\Omega} - \boldsymbol{\Omega}_c$ . In addition, the tracking error of the angular rates is also defined as  $\mathbf{e}_2 = \boldsymbol{\omega} - \boldsymbol{\omega}_c$ , where the desired angular rates  $\boldsymbol{\omega}_c$  can be obtained from the controller of the attitude angles. According to the above, a coordinated scheme based on the coordinated factors is given in Fig. 1.

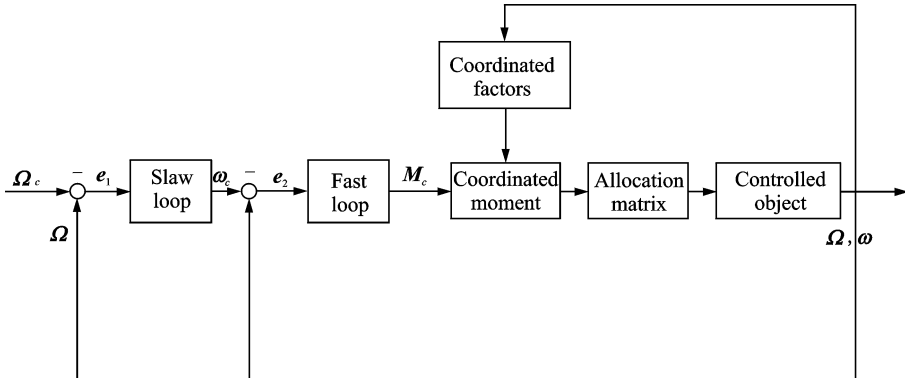


Fig. 1 Coordinated schematic diagram

#### 4.1 Slow loop controller design

The sliding mode surface is given as

$$\boldsymbol{\sigma} = \mathbf{e}_1 + \mathbf{K} \int_0^t \mathbf{e}_1 dt \quad (27)$$

where  $\mathbf{K} = \text{diag}\{K_1, K_2, K_3\}$ ,  $K_i > 0, i = 1, 2, 3$ .

The derivative of the sliding mode function can be obtained as follows

$$\begin{aligned} \dot{\boldsymbol{\sigma}} &= \dot{\mathbf{e}}_1 + \mathbf{K} \mathbf{e}_1 = \\ & \mathbf{f}_1 + \boldsymbol{\Psi}^T \boldsymbol{\theta}_\Omega + \mathbf{g}_s \boldsymbol{\omega} - \dot{\boldsymbol{\Omega}}_c + \mathbf{K} \mathbf{e}_1 = \\ & \mathbf{f}_1 + \boldsymbol{\Psi}^T \boldsymbol{\theta}_\Omega + \mathbf{g}_s (\mathbf{e}_2 + \boldsymbol{\omega}_c) - \dot{\boldsymbol{\Omega}}_c + \mathbf{K} \mathbf{e}_1 \end{aligned} \quad (28)$$

And, we can obtain

$$\boldsymbol{\omega}_c = -\mathbf{g}_s^{-1} (\boldsymbol{\kappa}_1 \boldsymbol{\sigma} + \mathbf{f}_1 + \boldsymbol{\Psi}^T \hat{\boldsymbol{\theta}}_\Omega - \dot{\boldsymbol{\Omega}}_c + \mathbf{K} \mathbf{e}_1) \quad (29)$$

Similar to Ref. [32], the adaptation law of  $\boldsymbol{\theta}_\Omega$  is designed as

$$\dot{\boldsymbol{\theta}}_\Omega = \text{Proj}_{\hat{\boldsymbol{\theta}}_\Omega} (\boldsymbol{\Gamma}_1 (\boldsymbol{\Psi} \boldsymbol{\sigma} - \boldsymbol{\lambda}_\Omega \tilde{\boldsymbol{\theta}}_\Omega)) \quad (30)$$

where  $\boldsymbol{\kappa}_1 > 0, \boldsymbol{\Gamma}_1 \in \mathbf{R}^{4 \times 4}, \boldsymbol{\lambda}_\Omega = \text{diag}\{\lambda_1, \lambda_2, \lambda_3, \lambda_4\} > 0$ .

Consider a Lyapunov function candidate as

$$V_1 = \frac{1}{2} \boldsymbol{\sigma}^T \boldsymbol{\sigma} + \frac{1}{2} \tilde{\boldsymbol{\theta}}_\Omega^T \boldsymbol{\Gamma}_1^{-1} \tilde{\boldsymbol{\theta}}_\Omega \quad (31)$$

The time derivative of Eq. (31) is

$$\begin{aligned} \dot{V}_1 &= \boldsymbol{\sigma}^T (\mathbf{f}_1 + \boldsymbol{\Psi}^T \boldsymbol{\theta}_\Omega + \mathbf{g}_s (\mathbf{e}_2 + \boldsymbol{\omega}_c) - \dot{\boldsymbol{\Omega}}_c + \mathbf{K} \mathbf{e}_1) + \\ & \tilde{\boldsymbol{\theta}}_\Omega^T \boldsymbol{\Gamma}_1^{-1} \text{Proj}_{\hat{\boldsymbol{\theta}}_\Omega} (\boldsymbol{\Gamma}_1 (\boldsymbol{\Psi} \boldsymbol{\sigma} - \boldsymbol{\lambda}_\Omega \tilde{\boldsymbol{\theta}}_\Omega)) \end{aligned} \quad (32)$$

From Eqs. (29), (30), (32), we can obtain

$$\begin{aligned} \dot{V}_1 &= -\boldsymbol{\kappa}_1 \boldsymbol{\sigma}^T \boldsymbol{\sigma} + \boldsymbol{\sigma}^T \mathbf{g}_s \mathbf{e}_2 + \boldsymbol{\sigma}^T \boldsymbol{\Psi}^T \boldsymbol{\theta}_\Omega - \\ & \boldsymbol{\sigma}^T \boldsymbol{\Psi}^T \hat{\boldsymbol{\theta}}_\Omega + \tilde{\boldsymbol{\theta}}_\Omega^T \boldsymbol{\Gamma}_1^{-1} \cdot \text{Proj}_{\hat{\boldsymbol{\theta}}_\Omega} (\boldsymbol{\Gamma}_1 (\boldsymbol{\Psi} \boldsymbol{\sigma} - \boldsymbol{\lambda}_\Omega \tilde{\boldsymbol{\theta}}_\Omega)) = \\ & -\boldsymbol{\kappa}_1 \boldsymbol{\sigma}^T \boldsymbol{\sigma} + \boldsymbol{\sigma}^T \mathbf{g}_s \mathbf{e}_2 - \boldsymbol{\sigma}^T \boldsymbol{\Psi} \tilde{\boldsymbol{\theta}}_\Omega + \\ & \tilde{\boldsymbol{\theta}}_\Omega^T \boldsymbol{\Gamma}_1^{-1} \text{Proj}_{\hat{\boldsymbol{\theta}}_\Omega} (\boldsymbol{\Gamma}_1 (\boldsymbol{\Psi} \boldsymbol{\sigma} - \boldsymbol{\lambda}_\Omega \tilde{\boldsymbol{\theta}}_\Omega)) \leq \\ & -\boldsymbol{\kappa}_1 \boldsymbol{\sigma}^T \boldsymbol{\sigma} + \boldsymbol{\sigma}^T \mathbf{g}_s \mathbf{e}_2 - \tilde{\boldsymbol{\theta}}_\Omega^T \boldsymbol{\lambda}_\Omega \tilde{\boldsymbol{\theta}}_\Omega \end{aligned} \quad (33)$$

#### 4.2 Fast loop controller design

Differentiating  $\mathbf{e}_2$  yields

$$\dot{\mathbf{e}}_2 = \dot{\boldsymbol{\omega}} - \dot{\boldsymbol{\omega}}_c = \boldsymbol{\Xi}^T \boldsymbol{\theta}_\omega + \mathbf{g}_f \mathbf{M}_c + \mathbf{d} - \dot{\boldsymbol{\omega}}_c \quad (34)$$

Then, the control law  $\mathbf{M}_c$  is designed as

$$\mathbf{M}_c = -\mathbf{g}_f^{-1} (\boldsymbol{\kappa}_2 \mathbf{e}_2 + \boldsymbol{\Xi}^T \boldsymbol{\theta}_\omega + \hat{\mathbf{d}} + \mathbf{g}_f^T \boldsymbol{\sigma} - \dot{\boldsymbol{\omega}}_c) \quad (35)$$

where  $\hat{\mathbf{d}}$  is the estimate output of the disturbance observer. The disturbance estimation error  $\tilde{\mathbf{d}}$  is defined as  $\tilde{\mathbf{d}} = \mathbf{d} - \hat{\mathbf{d}}$ . And the adaptation law of  $\hat{\boldsymbol{\theta}}_\omega$

is chosen as

$$\dot{\hat{\boldsymbol{\theta}}}_\omega = \text{Proj}_{\hat{\boldsymbol{\theta}}_\omega} (\boldsymbol{\Gamma}_2 (\boldsymbol{\Xi} \mathbf{e}_2 - \boldsymbol{\lambda}_\omega \tilde{\boldsymbol{\theta}}_\omega)) \quad (36)$$

where  $\boldsymbol{\kappa}_2 > 0, \boldsymbol{\Gamma}_2 \in \mathbf{R}^{17 \times 17} > 0$ , and  $\boldsymbol{\lambda}_\omega \in \mathbf{R}^{17 \times 17} > 0$ .

According to Refs. [32–36], the disturbance observer is designed as

$$\begin{cases} \dot{\hat{\mathbf{d}}} = \mathbf{z} + \mathbf{Q}(\mathbf{e}) \\ \dot{\mathbf{z}} = -\mathbf{L}(\mathbf{e}) \mathbf{z} - \mathbf{L}(\mathbf{e}) (\boldsymbol{\Xi}^T \hat{\boldsymbol{\theta}}_\omega + \mathbf{g}_f \mathbf{M} + \mathbf{Q}(\mathbf{e})) \end{cases} \quad (37)$$

where  $\mathbf{z} = \hat{\mathbf{d}} - \mathbf{Q}(\mathbf{e})$ ,  $\mathbf{Q}(\mathbf{e}) = [q_1(\mathbf{e}), q_2(\mathbf{e}), \dots, q_n(\mathbf{e})]^T \in \mathbf{R}^n$ ,  $\mathbf{L}(\mathbf{e}) = \frac{\partial \mathbf{Q}(\mathbf{e})}{\partial \mathbf{e}}$ .

**Remark 2** Different from Ref. [33], the designed observer exists the uncertain parameters estimation vector  $\hat{\boldsymbol{\theta}}_\omega$ , so the convergence of the observer should be considered. At the origin,  $\tilde{\boldsymbol{\theta}}_\omega$  is asymptotic stable if  $\boldsymbol{\theta}_\omega$  is convergent. In Eq. (37),  $\hat{\boldsymbol{\theta}}_\omega$  can be written as  $\boldsymbol{\theta}_\omega + \tilde{\boldsymbol{\theta}}_\omega$ , then  $\tilde{\boldsymbol{\theta}}_\omega = 0$ , and Eq. (37) is simplified as the form of Ref. [33]. So the convergence of Eq. (37) depends on the convergence of the adaptive estimator, and the asymptotic stability of the adaptive estimator will be proved in the next.

**Theorem 1** For the attitude dynamics in Eq. (20), under the control laws (29) and (35), with the adaptive laws (30) and (36), the designed scheme guarantees that all signals of the closed-loop system are uniformly and fully bounded and the tracking errors are asymptotically stable.

**Proof** Consider a Lyapunov function candidate as follows

$$\mathbf{V} = V_1 + \frac{1}{2} (\mathbf{e}_2^T \mathbf{e}_2 + \tilde{\boldsymbol{\theta}}_\omega^T \boldsymbol{\Gamma}_2^{-1} \tilde{\boldsymbol{\theta}}_\omega + \tilde{\mathbf{d}}^T \tilde{\mathbf{d}}) \quad (38)$$

Then, the time derivative of  $\mathbf{V}$  is

$$\dot{\mathbf{V}} = \dot{V}_1 + \mathbf{e}_2^T \dot{\mathbf{e}}_2 + \tilde{\boldsymbol{\theta}}_\omega^T \boldsymbol{\Gamma}_2^{-1} \dot{\tilde{\boldsymbol{\theta}}}_\omega + \tilde{\mathbf{d}}^T \dot{\tilde{\mathbf{d}}} \quad (39)$$

Substituting Eqs. (33)–(35), (36) into Eq. (39) and considering that the disturbance's change frequency is very small, that is  $\dot{\mathbf{d}} \approx 0$ , we have

$$\begin{aligned} \dot{\mathbf{V}} &\leq -\boldsymbol{\kappa}_1 \boldsymbol{\sigma}^T \boldsymbol{\sigma} + \boldsymbol{\sigma}^T \mathbf{g}_s \mathbf{e}_2 - \tilde{\boldsymbol{\theta}}_\Omega^T \boldsymbol{\lambda}_\Omega \tilde{\boldsymbol{\theta}}_\Omega + \\ & \mathbf{e}_2^T (\boldsymbol{\Xi}^T \boldsymbol{\theta}_\omega + \mathbf{g}_f \mathbf{M}_c + \end{aligned}$$

$$\begin{aligned}
& \mathbf{d} - \dot{\boldsymbol{\omega}}_c) + \tilde{\boldsymbol{\theta}}_\omega^\top \boldsymbol{\Gamma}_2^{-1} \text{Proj}_{\tilde{\boldsymbol{\theta}}_\omega} (\boldsymbol{\Gamma}_2 (\boldsymbol{\Xi} \mathbf{e}_2 - \boldsymbol{\lambda}_\omega \tilde{\boldsymbol{\theta}})) + \tilde{\mathbf{d}}^\top \dot{\mathbf{d}} \leq \\
& -\boldsymbol{\kappa}_1 \boldsymbol{\sigma}^\top \boldsymbol{\sigma} - \tilde{\boldsymbol{\theta}}_\Omega^\top \boldsymbol{\lambda}_\Omega \tilde{\boldsymbol{\theta}}_\Omega - \boldsymbol{\kappa}_2 \mathbf{e}_2^\top \mathbf{e}_2 - \tilde{\boldsymbol{\theta}}_\omega^\top \boldsymbol{\lambda}_\omega \tilde{\boldsymbol{\theta}}_\omega + \tilde{\mathbf{d}}^\top \dot{\mathbf{d}} \leq \\
& -\boldsymbol{\kappa}_1 \boldsymbol{\sigma}^\top \boldsymbol{\sigma} - \tilde{\boldsymbol{\theta}}_\Omega^\top \boldsymbol{\lambda}_\Omega \tilde{\boldsymbol{\theta}}_\Omega - \boldsymbol{\kappa}_2 \mathbf{e}_2^\top \mathbf{e}_2 - \tilde{\boldsymbol{\theta}}_\omega^\top \boldsymbol{\lambda}_\omega \tilde{\boldsymbol{\theta}}_\omega - \tilde{\mathbf{d}}^\top \mathbf{L} \dot{\mathbf{d}}
\end{aligned} \quad (40)$$

Denote  $\mathbf{L}(\mathbf{e}) = c > 1$  and  $\mathbf{Q}(\mathbf{e}) = c\mathbf{e}$ , it can be obtained that

$$\begin{aligned}
\dot{\mathbf{V}} \leq & -\boldsymbol{\kappa}_1 \boldsymbol{\sigma}^\top \boldsymbol{\sigma} - \tilde{\boldsymbol{\theta}}_\Omega^\top \boldsymbol{\lambda}_\Omega \tilde{\boldsymbol{\theta}}_\Omega - \boldsymbol{\kappa}_2 \mathbf{e}_2^\top \mathbf{e}_2 - \tilde{\boldsymbol{\theta}}_\omega^\top \boldsymbol{\lambda}_\omega \tilde{\boldsymbol{\theta}}_\omega - \\
& (c-1) \|\tilde{\mathbf{d}}\|^2 \leq 0
\end{aligned} \quad (41)$$

Eqs. (39), (41) confirm that the signals  $\boldsymbol{\sigma}, \tilde{\boldsymbol{\theta}}_\Omega, \tilde{\boldsymbol{\theta}}_\omega, \tilde{\mathbf{d}}, \mathbf{e}_2$  are bounded since  $\dot{\mathbf{V}}$  is negative semi-definite. From Eq. (27), we know that  $\mathbf{e}_1$  is bounded. Then Eq. (41) can be written as

$$\mathbf{V}_i(t) \leq -\zeta_i e_i^2(t) \quad i=1,2 \quad (42)$$

where  $\zeta_i > 0$ , and  $\mathbf{e}_i(t)$  is the tracking error. By integrating (42) from 0 to  $\infty$ , we have

$$\int_0^\infty \zeta_i e_i^2(t) dt \leq -\int_0^\infty \dot{\mathbf{V}}_i(t) dt = \mathbf{V}_i(0) - \mathbf{V}_i(\infty) \quad (43)$$

This implies that  $e_i(t) \in L_2$ , since  $\mathbf{V}_i(0)$  and  $\mathbf{V}_i(\infty)$  are bounded. Since  $e_i(t) \in L_\infty$ ,  $\dot{e}_i(t) \in L_\infty$ ,  $e_i(t) \in L_2$ , we can conclude that  $\lim_{t \rightarrow \infty} e_i(t) = 0$  by using Barbalat's lemma. Therefore, the tracking error  $e_i(t)$  is ultimately and asymptotically stable, i. e.,  $\lim_{t \rightarrow \infty} e_i(t) = 0$ .

### 4.3 Coordinated implement

The objective of the coordinated control is first to calculate the coordinated moment by using the coordinated factors and the control moment  $\mathbf{M}_c$ , and then to allocate the coordinated moment to the deflection angles of the elevator, the aileron, and the rudder, respectively.

Considering the coordinated factor in Eq. (19), the attitude control moment  $\mathbf{M}_c$ , and the allocation matrix  $\mathbf{g}_{f\delta}$  of the fast-loop, the coordinated moment can be obtained as follows

$$\mathbf{M}_c = \mathbf{g}_{f\delta} \boldsymbol{\delta} \quad (44)$$

where

$$\begin{aligned}
\mathbf{g}_{f\delta} = & \mathbf{g}_{f\delta} + \boldsymbol{\Gamma} = \\
& \begin{bmatrix} \mathbf{g}_{p,\delta_e} + \lambda_e & \mathbf{g}_{p,\delta_a} & \mathbf{g}_{p,\delta_r} \\ \mathbf{g}_{q,\delta_e} & \mathbf{g}_{q,\delta_a} + \lambda_a & \mathbf{g}_{q,\delta_r} \\ \mathbf{g}_{r,\delta_e} & \mathbf{g}_{r,\delta_a} & \mathbf{g}_{r,\delta_r} + \lambda_r \end{bmatrix}
\end{aligned} \quad (45)$$

By using Eqs. (44), (45), we have

$$\boldsymbol{\delta} = \mathbf{g}_{f\delta}^{-1} \boldsymbol{\delta} \cdot \mathbf{M}_c \quad (46)$$

According to Eq. (18), when the control strategy is using the elevator deflection to implement the pitch moment and using the coordinated deflections of the aileron and rudder to implement the yaw and roll moments, Eq. (47) can be obtained

$$\delta_{\text{coe}} = \delta_e, \delta_{\text{coa}} = E\delta_r, \delta_{\text{cor}} = \delta_r \quad (47)$$

## 5 Simulation and Analysis

The initial values of the simulation study are chosen as  $V_0 = 2200$  m/s,  $H_0 = 21000$  m,  $\alpha = 1^\circ$ ,  $\beta = 5^\circ$ ,  $\mu = 0$ ,  $p = q = r = 0$  °/s, and the desired flight attitude angles are chosen as  $\alpha_c = 5^\circ$ ,  $\beta_c = 0^\circ$ ,  $\mu_c = 4^\circ$ .

Suppose that there are +20% and -20% uncertainties on the aerodynamic coefficients and the aerodynamic moment coefficients, respectively. And the unknown external disturbance  $\mathbf{D}$  is given as

$$\mathbf{D}(t) = 10 \times [0.5 \sin(1.5t) \quad 0.5 \cos(2t) \quad 0.5 \sin(2t)]^\top$$

The design parameters of the attitude controller are chosen as  $k_i = 1$ ,  $i = 1, \dots, 7$ ,  $K_1 = K_2 = K_3 = 4$ , and  $\boldsymbol{\kappa}_1 = \boldsymbol{\kappa}_2 = 5$ .

The simulation results of the attitude angles are shown in Fig. 2. The overshoot of uncoordinated  $\alpha$  is 35% and that of coordinated  $\alpha$  is 10%. The overshoot of the coordinated  $\beta$  is less than the uncoordinated  $\beta$ . The simulation result of  $\mu$  is similar to  $\beta$ , which demonstrates that the performance of the coordinated attitude controller is superior to the uncoordinated one. It is obvious that the advantages of the coordinated factor in Eq. (13) lie in the smaller overshoot, less jitter, faster response, and quicker stabilization process. From Fig. 3, we can find that the angular rates can approach the equilibrium more quickly, resulted from the coordinated controller, which shows that the coordinated factor in Eq. (14) ensures that the jitter times are kept in a small range. In Fig. 4, by using the coordinated strategy of Eq. (47), it promotes the efficiency of the control

surface deflection. And this performance improvement can enhance the control-ability of the attitude system and the maneuverability of the hypersonic flight vehicle.

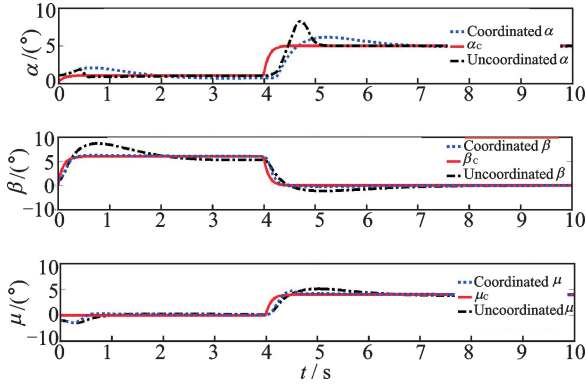


Fig. 2 Tracking responses of  $\alpha, \beta, \mu$

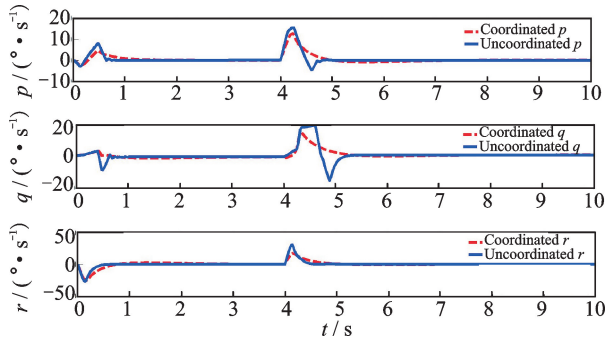


Fig. 3 Tracking responses of  $p, q,$  and  $r$

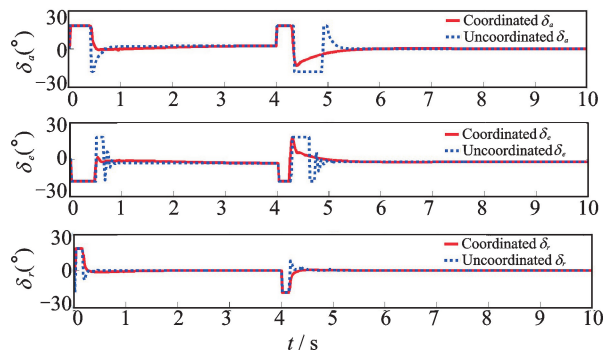


Fig. 4 Tracking responses of  $\delta_a, \delta_e$  and  $\delta_c$

## 6 Conclusions

This study indicates that, although the flight condition of a type of hypersonic aircraft contains strong couplings and uncertain disturbances, the design controllers can effectively compensate the effect of the compound disturbance and suppress the coupling phenomena. The definition of the

coordinated factors provides a new solution to deal with the complex nonlinear relationships of the coupling variables. The proposed method provides the coupling analysis based on the flight dynamics, as well as analytical expressions, which can help to achieve satisfied tracking performance. In further studies, the robust coordinated control of the longitudinal dynamics of hypersonic aircraft will be discussed.

## Acknowledgements

This work was supported by the National Natural Science Foundation of China (Nos. 61773204, 61374212).

## References:

- [1] WU H X, MENG B. Review on the control of hypersonic flight vehicles [J]. *Advances in Mechanics*, 2009, 39(6): 756-765.
- [2] XU B, SHI Z K. An overview on flight dynamics and control approaches for hypersonic vehicles [J]. *Science China Information Sciences*, 2015, 58(7): 1-19.
- [3] KESHMIRI S, MIRMIRANI M, COLGREN R. Six-DOF modeling and simulation of a generic hypersonic vehicle for conceptual design studies [C]// *AIAA modeling and simulation technologies conference and exhibit*. Rhode Island, USA: AIAA, 2004: 1-12.
- [4] CHENG K, LIU K. Dynamic inversion based hypersonic vehicle attitude sliding mode control [C]// *2015 IEEE International Conference on Information and Automation*. Lijiang, China: IEEE, 2015: 2848-2852.
- [5] KANG S, KIM H J, LEE J I. Roll-pitch-yaw integrated robust autopilot design for a high angle-of-attack missile [J]. *Journal of Guidance, Control and Dynamics*, 2009, 32(5): 1622-1628.
- [6] PARKER J T, SERRANI A, YURKOVICH S. Control-oriented modeling of air-breathing hypersonic vehicle [J]. *Journal of Guidance, Control, and Dynamics*, 2007, 30(3): 856-869.
- [7] ZIMPFER D, SHIEH L, SUNKEL J. Digitally redesigned pulse-width modulation spacecraft control [J]. *Journal of Guidance, Control and Dynamics*, 1998, 21(4): 529-534.
- [8] THURMAN S, FLASHNER H. Robust digital autopilot design for spacecraft equipped with pulse-operated thrusters [J]. *Journal of Guidance, Control and Dynamics*, 2012, 19(5): 1047-1055.
- [9] DAS K, PURLUPADAY C, PADHI R, et al. Opti-

- mal nonlinear control and estimation for a reusable launch vehicle during reentry phase[C]//Proceedings of the 16th Mediterranean Conference on Control and Automation. Ajaccio-Corsica, France: IEEE, 2008: 47-52.
- [10] SHTESSEL Y, KRUPP D. Reusable launch vehicle trajectory control in sliding modes[C]//Proceeding of the 1997 American Control Conference. USA: [s. n.], 1997: 2557-2561.
- [11] YU X, MAN Z. Fast terminal sliding-mode control design for nonlinear dynamical systems [J]. IEEE Transactions on Circuits and Systems-I, Fundamental Theory and Applications, 2002, 49(2): 261-264.
- [12] CHEN M, JIANG B. Robust attitude control of near space vehicles with time-varying disturbances [J]. International Journal of Control, Automation and Systems, 2013, 11(1): 182-187.
- [13] LUO X, LI J. Fuzzy dynamic characteristic model based attitude control of hypersonic vehicle in gliding phase [J]. Science China Information Sciences, 2011, 54(3): 448-459.
- [14] HELLER M, SACHS G, GUNNARSSON K, et al. Flight dynamics and robust control of a hypersonic test vehicle with ramjet propulsion [C]//Proceedings of the 8th AIAA International Space Planes and Hypersonic Systems and Technologies Conference. [S. l.]:AIAA, 1998: 3-10.
- [15] FEZZANI A, DRID S, MAKOUF A, et al. Speed sensorless flatness-based control of PMSW using a second order sliding mode observer [C]//The 8th International Conference and Exhibition on Ecological Vehicles and Renewable Energies. [S. l.]: IEEE, 2013: 1-9.
- [16] SURYAWANSHI P V, SHENDGE P D, PHADKE S B. Robust sliding mode control for a class of nonlinear systems using inertial delay control [J]. Nonlinear Dynamics, 2014, 78(3): 1921-1932.
- [17] BESSA W M, DUTRA M S, KREUZER E. Sliding mode control with adaptive fuzzy dead-zone compensation of an electro-hydraulic servo-system [J]. Journal of Intelligent and Robotic Systems, 2010, 58(1): 3-16.
- [18] SIRA-RAMIREZ H, ZRIBI M, AHMAD S. Dynamical sliding mode control approach for vertical flight regulation in helicopters [J]. Control Theory Application, 2002, 141(1): 19-24.
- [19] WANG W, GUO R. Study of flow characteristics of hypersonic inlet based on boundary layer transition [J]. Acta Aeronautical et Astronautica Sinica, 2012, 33(10): 1772 -1780.
- [20] TORREZ S M, DRISCOLL J F, DALLE D J. Scramjet engine model MASIV: Role of mixing, chemistry and wave interaction [C]//Proceeding of the 45th AIAA/ASME/SAE/ASEE Joint Propulsion Conference and Exhibit. Denver, USA: AIAA, 2009: 121-127.
- [21] TORREZ S M, SCHOLTEN N A, MICKA D J, et al. A scramjet engine model including effects of pre-combustion shocks and dissociation [C]//Proceeding of the 44th AIAA/ASME/SAE/ASEE Joint Propulsion Conference and Exhibit. Hartford, USA: AIAA, 2008:1-22.
- [22] WU H, HU J, XIE Y. Characteristic model-based all-coefficient adaptive control method and its applications [J]. IEEE Transactions on Systems Man and Cybernetics, Part C, 2007, 37(2): 213-221.
- [23] ZHANG J. Robust adaptive control for nonlinear uncertain flight moving systems of near space vehicle [D]. Nanjing: Nanjing University of Aeronautics and Astronautics, Nanjing, 2009. (in Chinese)
- [24] HSIEH C T, WU Q, DING C S, et al. Statistical sampling and regression analysis for RT-level power evaluation [C]//Proceedings of the 1996 IEEE/ACM International Conference on Computer-Aided Design. USA: IEEE Computer Society, 1997: 583-588.
- [25] ZHOU J, ZHOU M, LIN P. Research on the control-configured optimization to reduce aerodynamic nonlinearity of hypersonic vehicles [J]. Journal of Astronautics, 2012, 33(7): 870-875.
- [26] MIAO R S, JU X M, WU J S. Missile aerodynamics [M]. Beijing: National Defense Industry Press, 2006: 500-519. (in Chinese)
- [27] GENG J, SHENG Y, LIU X. Second-order time-varying sliding mode control for reentry vehicle [J]. International Journal of Intelligent Computing and Cybernetics, 2013, 6(3): 272-295.
- [28] FU J, WANG L, CHEN M, et al. Robust Adaptive attitude control for air-breathing hypersonic vehicle with attitude constraints and propulsive disturbance [J]. Mathematical Problem in Engineering, 2015, 2015(2): 1-11.
- [29] JIN K, LUO J, SU E, et al. Double-loop coordinated decoupling and control for gliding hypersonic vehicles [J]. Journal of Northwestern Polytechnical University, 2014, 32(3):440-445. (in Chinese)
- [30] ZHEN W, WANG Y, WU Q, et al. Coordinated attitude control of hypersonic flight vehicles based on the coupling analysis [J]. Proceedings of the Institu-

tion of Mechanical Engineers Part G Journal of Aerospace Engineering, 2018, 232(5): 1002-1011.

- [31] ZHOU M, ZHOU J, LIN P. A new method of hypersonic vehicle configuration control and optimization for reducing control coupling of aerodynamic rudder [J]. Journal of Northwestern Polytechnical University, 2014, 32(1): 1-5. (in Chinese)
- [32] XU L, YAO B. Output feedback adaptive robust precision motion control of linear motors [J]. Automatica, 2001, 37(7): 1029-1039.
- [33] YANG Z, MENG B, SUN H. A new kind of nonlinear disturbance observer for nonlinear systems with applications to cruise control of air-breathing hypersonic vehicles [J]. International Journal of Control, 2017, 90(9): 1935-1950.
- [34] CHEN M, YU J. Disturbance observer-based adaptive sliding mode control for near-space vehicles [J]. Nonlinear Dynamics, 2015, 82(4): 1671-1682.
- [35] GUO Z, ZHOU J, GUO J, et al. Coupling-characterization-based robust attitude control scheme for hypersonic vehicles [J]. IEEE Transactions on Industrial Electronics, 2017, 64(8): 6350-6361.
- [36] GUO Z Y, ZHOU J, GUO J G. Novel coupling based attitude control system design for hypersonic vehicles [J]. Journal of Astronautics, 2017, 38(3): 270-278.

Mr. **Mu Jinzhen** received the B. S. degree in automation from Inner Mongolia University of Technology in 2014 and M. S. degree in control engineering from Nanjing University of Aeronautics and Astronautics in 2018, respectively.

From 2014 to 2015, he was an engineer of the Shandong Electric Power Construction Third Engineering Company. From April 2018 to present, he joined Shanghai Aerospace Control Technology Institute, where he is currently a full researcher and development engineer. His research has focused on flight control, coordinated control, and relevant fields.

Dr. **Wang Yuhui** received the B. S. and M. S. degrees in automation from Jinan University, Jinan, China, in 2001 and 2004, respectively. In 2008, she received Ph. D degree in control theory and control engineering from Nanjing University of Aeronautics and Astronautics (NUAA). In July 2008, she joined in Nanjing University of Aeronautics and Astronautics. At present, she is an associate professor of College of Automation Engineering, NUAA. Her research is focused on hypersonic aircraft, flight control, and fire control.

Prof. **Wu Qingxian** received M. S. degree in control theory and control engineering in Southeast University in 1985. From 1985, he has worked at the College of Automation Engineering, Nanjing University of Aeronautics and Astronautics, Nanjing, China. His research interests include nonlinear control, robust control, and adaptive control.

Mr. **Ying Junyu** received the M. S. degree in control engineering from Nanjing University of Aeronautics and Astronautics in 2018. From April 2018 to present, he has worked at Nuctech Company Limited, Nanjing, China, where he is currently a full researcher and development engineer. His research has focused on reliability control, and damage mitigating control.

(Executive Editor; Zhang Bei)